Accepted Manuscript

Damage to inner ear structure during cochlear implantation: Correlation between insertion force and radio-histological findings in temporal bone specimens

Daniele De Seta, Renato Torres, Francesca Yoshie Russo, Evelyne Ferrary, Guillaume Kazmitcheff, Dominique Heymann, Jerome Amiaud, Olivier Sterkers, Daniele Bernardeschi, Yann Nguyen

PII: S0378-5955(16)30334-3

DOI: 10.1016/j.heares.2016.11.002

Reference: HEARES 7267

To appear in: *Hearing Research*

Received Date: 31 July 2016

Revised Date: 13 October 2016

Accepted Date: 3 November 2016

Please cite this article as: De Seta, D., Torres, R., Russo, F.Y., Ferrary, E., Kazmitcheff, G., Heymann, D., Amiaud, J., Sterkers, O., Bernardeschi, D., Nguyen, Y., Damage to inner ear structure during cochlear implantation: Correlation between insertion force and radio-histological findings in temporal bone specimens, *Hearing Research* (2016), doi: 10.1016/j.heares.2016.11.002.

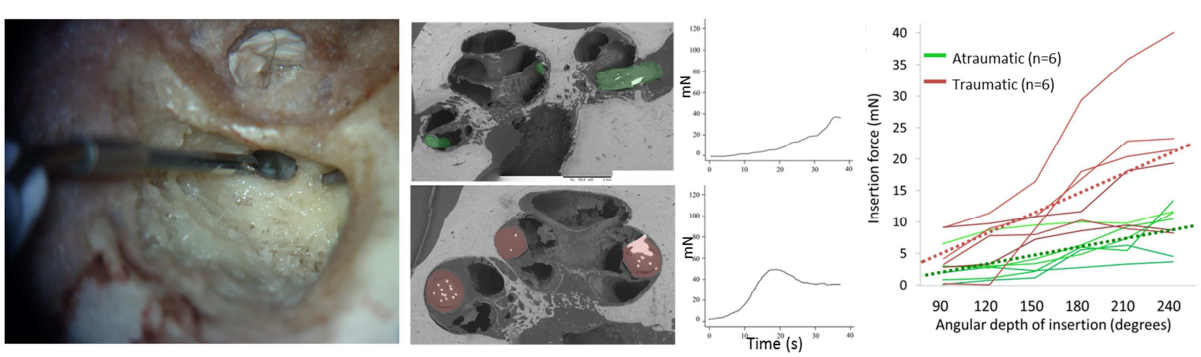

Damage to inner ear structure during cochlear implantation: Correlation between insertion force and radio-histological findings in temporal bone specimens

Daniele De Seta[a,b,c], Renato Torres[a], Francesca Yoshie Russo[a,b,c], Evelyne Ferrary[a], Guillaume Kazmitcheff[a], Dominique Heymann[d,e], Jerome Amiaud[e], Olivier Sterkers[a,b], Daniele Bernardeschi[a,b], Yann Nguyen[a,b]

[a] Sorbonne Universités, Université Pierre et Marie Curie Paris 6, Inserm, Unité Réhabilitation chirurgicale mini-invasive et robotisée de l'audition, Paris, France

[b] AP-HP, GHU Pitié-Salpêtrière, Service ORL, Otologie, implants auditifs et chirurgie de la base du crâne, Paris, France

[c] Department of Sense Organs, Sapienza University of Rome, Rome, Italy

[d] INSERM UMR 957, "Pathophysiology of Bone Resorption and Therapy of Primary Bone Tumors", Nantes, France

[e] Department of Oncology and Metabolism, University of Sheffield, The Medical School, England

Corresponding author: Daniele De Seta

This research did not receive any specific grant from funding agencies in the public, commercial, or not-for-profit sectors.

Abstract

Cochlear implant insertion should be as least traumatic as possible in order to reduce trauma to the cochlear sensory structures. The force applied to the cochlea during array insertion should be controlled to limit insertion-related damage. The relationship between insertion force and histological traumatism remains to be demonstrated. Twelve freshly frozen cadaveric temporal bones were implanted **with a long straight electrodes array through an anterior extended round window insertion** using a motorized insertion tool with real-time measurement of the insertion force. Anatomical parameters, measured on a pre-implantation cone beam CT scan, position of the array and force metrics were correlated with post-implantation scanning electron microscopy images and histological damage assessment. An atraumatic insertion occurred in six cochleae, a translocation in five cochleae and a basilar membrane rupture in one cochlea. The translocation always occurred in the 150- to 180-degree region. In the case of traumatic insertion, different force profiles were observed with a more irregular curve arising from the presence of an early peak force (30 ± 18.2 mN). This corresponded approximately to the first point of contact of the array with the lateral wall of the cochlea. Atraumatic and traumatic insertions had significantly different force values at the same depth of insertion ($p < 0.001$, two-way ANOVA), and significantly different regression lines ($y = 1.34x + 0.7$ for atraumatic and $y = 3.37x + 0.84$ for traumatic insertion, $p < 0.001$, ANCOVA). In the present study, the insertion force was correlated with the intracochlear trauma. The 150- to 180-degree region represented the area at risk for scalar translocation **for this straight electrodes array**. Insertion force curves with different sets of values were identified for traumatic and atraumatic insertions; these values should be considered during motorized insertion of an implant so as to be able to modify the insertion parameters (e.g axis of insertion) and facilitate preservation of endocochlear structures.

Keywords: cochlear implant, insertion force, inner ear traumatism, scanning electron microscopy, histology, temporal bone

1. Introduction

Over the past decade, the indications for cochlear implantation have changed and broadened from bilateral profound deafness towards hearing loss involving only high frequencies or single sided deafness. As a consequence, surgery has evolved toward a low intracochlear trauma insertion in order to maintain the integrity of inner ear structures in all cochlear implant (CI) recipients, even those destined for electric-only stimulation. Indeed, the reduction in traumatism during implantation may offer several advantages. In patients with functional preimplant low-frequency hearing, minimizing the trauma can allow preservation of residual hearing and electric-acoustic stimulation. For all other patients, reducing intracochlear damage may limit fibrosis and ossification, making revision surgery for device failure or upgrade easier; this is particularly important for pediatric patients, who, during their lifetime, have an increased possibility that reimplantation will be required. Moreover, limiting injury potentially allows for the application of future technologies, such as cellular regeneration or other novel cochlear nerve stimulation technologies (Carlson et al., 2011). The concept of soft surgery was introduced by Lehnhardt (1993), and since then, CI centers have begun to follow this surgical technique in all cochlear implantations regardless of the necessity to preserve hearing or not. In parallel, CI manufacturers have modified the electrode array shape and physical characteristics making them thinner, more flexible, and in some cases shorter.

Short electrode arrays are less traumatic for inner ear structures (Lenarz et al., 2006), and the force applied during insertion of a shorter array is lower than for longer ones (Briggs et al., 2011). Nevertheless, a disadvantage of short electrode arrays is the limited low-frequency stimulation, especially in the case of loss of residual hearing, which may require reimplantation with a longer array (Nguyen et al., 2013).

Considering straight or precurved electrodes, effects on the lateral wall from straight electrodes were less traumatic than with precurved arrays (Briggs et al., 2011; Boyer et al., 2015), nevertheless other studies did not find any difference in terms of post-implantation hearing performance between straight or perimodiolar arrays (Doshi et al., 2015).

Positioning of the electrode in the scala tympani was reported to produce better results, compared to positioning in the scala vestibuli, in terms of speech recognition score in CI patients (Skinner et al., 2007; Aschendorff et al., 2007; Holden et al., 2013); however, other studies found no difference in speech recognition (Wanna et al., 2011); nevertheless, a relationship was found between translocation and hearing preservation (Wanna et al., 2015).

In order to investigate insertion related trauma to inner ear structures, several authors have studied the forces applied to the cochlea during electrode array insertion. The influences of insertion speed,

use of lubricants, different electrode arrays, or different insertion tools on frictional forces have been reported so far (Nguyen et al., 2015; Miroir et al., 2012; Majdani et al., 2010; Rohani et al., 2014; Roland, 2005). At the present time, the relationship between insertion force and histological traumatism remains to be demonstrated. The aim of this work is to try to identify a correlation between the forces used during straight flexible electrode array insertion within the scala tympani and possible inner ear damage, and to estimate the maximal value of the force that should be applied to avoid damaging the inner ear structures.

2. Material and methods

Twelve freshly frozen cadaveric temporal bones (five pairs from five subjects and two single temporal bones) were prepared with a simple mastoidectomy and a posterior tympanotomy. A cone beam CT scan (CBCT) was performed on the temporal bone specimens before and after the insertion. The array (Flex 28 array, Med El, Innsbruck, Austria) was inserted at constant speed using a motorized insertion tool, and the frictional forces were recorded during insertion. The cochlea was extracted from the temporal bone for scanning electron microscope (SEM) imaging. Histological analysis was performed to confirm the position of the array and to study the inner ear structures. Between each of these steps, the temporal bones were frozen at -18 °C to ensure preservation of the structures. Each step is detailed below.

2.1 Cone beam CT scan imaging

The CBCT images were obtained with the NewTom 5G machine (NewTom 5G, QR s.r.l., Verona, Italy). The system set-up used a 200 x 25 mm flat panel detector at a distance of 650 mm from the radiation source. One 360-degree rotation of the X-ray tube took 36 seconds. The tube voltage was 110 kV, with a 19-mA charge at the terminals. Total filtrations were 2 mm, with a pitch of 125 µm; this corresponded to a field of view of 12 x 7.5 cm diameter. The images were isometric voxel rendered from the 125 µm sections.

The data from DICOM (Digital Imaging and Communications in Medicine) images were analyzed with Osirix software (Osirix v 4.0 64-bit; Pixmeo Sarl, Bernex, Switzerland). This program allowed multiplanar reconstructions for measurement of cochlear anatomy (De Seta et al., 2016). The major cochlear diameter (distance A) from the middle of the round window membrane to the opposite lateral wall (Escudé et al., 2006) was measured in the slice perpendicular to the modiolus axis and coplanar to the basal turn named the ‘cochlear view’ (Fig. 1A) (Xu et al., 2000); the cochlear height was measured from the cochlear fossa to the apex of the cochlea in a reformatted mid-modiolar plane perpendicular to the superior semicircular canal plane (Fig. 1B). The vertical and horizontal

diameters of the cochlear lumen were measured at 180- and 360-degrees (Fig. 1C). The angle between the first and second turns of the cochlea was measured between the axes of these two turns in a slice parallel to the superior semicircular canal (Martinez-Monedero et al., 2011) (Fig. 1D).

2.2 Cochlear implantation and insertion force measurement

The posterior rim of the round window niche was drilled in order to visualize the entire round window membrane; the membrane was subsequently removed with a sharp micro hook and the round window was enlarged anteriorly with removal of the crista fenestra. The temporal bone was fixed to an in-house constructed temporal bone holder coupled to a force sensor (ATI Nano 17, calibration type SI-12-0.12, resolution: 3 mN; ATI Industrial Automation, Apex, NC, USA). The electrode array was inserted through an extended inferior round window approach using a motorized insertion tool developed in a temporal bone research laboratory (Miroir et al., 2012) (Fig. 2). This tool comprised a rotary actuator (RE10CLL, MDP, Miribel, France) connected to a threaded screw that pushed a blunt pin into an insertion tube loading the array. The tool was held steady by a flexible arm. No force feedback loop was applied between this tool and the force sensor. The actuator speed was controlled via a laboratory power supply (Metrix AX 503, Chauvin-Arnoux, Paris, France) and set at 0.8 $mm \cdot s^{-1}$. The round window region was irrigated with saline serum, and sodium hyaluronate (Healon, Abbott Medical Optics, Abbott Park, IL, USA) was applied before the electrode array insertion. The frictional force between the array and the cochlea was measured with a 6-axis force sensor. Sensor data were recorded in real-time at a sampling rate of 100 Hz via the same analog-to-digital interface card that controlled the actuator input power. From the 6-axis sensor, insertion forces were computed based only on three linear force norms (Dx, Dy, Dz). The shape of the curve corresponding to force versus time was investigated. Four different metrics have been calculated: the peak force, the total change in momentum, the number of times when forces were increased by 50% within a small time step (sudden rise), and the smoothness of the curve, studied as "jerk" variation (expressed as $N \cdot s^{-1}$) (Nguyen et al., 2014).

2.3 Histological procedures

Immediately after its insertion, the electrode array was fixed to the round window region with cyanoacrylate glue to avoid any displacement during the subsequent steps. The cochlea was removed from the temporal bone and fixed in 10% buffered formalin. The specimen was successively dehydrated in graded alcohol and cast in methylmethacrylate resin (10% Polyethylene Glycol 400, 20% Technovit 7200 VLC, Heraeus Kultzer Gmbh, Germany; 70% methylmethacrylate).

The specimen was then cut (Leica SP 1660 Saw Microtome, Nussloch GmbH, Germany, sawing speed 3) perpendicular to the basal turn passing through the round window. A SEM acquisition (Hitachi TM

3000, Japan) was subsequently performed to identify the position of the electrodes, and each face of the resin bloc was also observed under a white light microscope. The half cochlea was subsequently ground to reach the apical electrode and a second acquisition with the SEM was performed. Damage to the inner ear structures was assessed using the cochlear trauma grading system published by Eshraghi et al. (2015): 0 represented no observable trauma; 1, elevation of the basilar membrane; 2, rupture of basilar membrane; 3, electrode in scala vestibuli; 4, severe trauma such as fracture of the osseous spiral lamina or modiolus or tear of the stria vascularis. The location of the trauma was also evaluated: A: lower basal turn (0 to 180 degrees), B: upper basal turn (181 to 360 degrees), C: lower middle turn (361 to 540 degrees), D: upper middle turn (541 to 720 degrees); E: apex (>721 degrees).

2.4 Statistical analysis

Results are expressed as mean ± standard deviation. Insertion force graphics were generated with "R" statistical software (http://www.r-project.org/). Spearman's rho correlation coefficient was used when appropriate. Two-way analysis of variance (ANOVA) [factors: traumatism (translocation, no translocation) and depth of insertion: (90-, 120-, 150-, 180-, 220-, 250-degrees)] was applied to analyze the insertion force across groups and depth of insertion. The difference in slope of the regression lines of the force for the two groups was tested by analysis of covariance (ANCOVA). All statistical analyses were performed using IBM SPSS for Windows (v 22.0, SPSS Inc., Chicago, IL, USA). For all comparisons, $p < 0.05$ was considered to be significant.

3. Results

The cochlear anatomy parameters and measurements of insertion forces are reported in Table 1. As expected, the cochlear height was correlated with the angle between the first and second turn ($r = 0.64$, $p=0.02$, data not shown); no other anatomic correlations were found. **Pre-insertion imaging analysis did not reveal any significant ossification or obvious obstruction of the cochlear lumen. During approach preparation, no fibrosis could be observed at the entrance of the basal turn under microscopic vision.** Ten electrode arrays were fully inserted whereas two insertions were incompletely inserted.

The histologic images and SEM images confirmed six atraumatic insertions, scalar translocation in five specimens (42%), and basilar membrane rupture without translocation in another insertion (Fig. 3). The scalar translocation occurred in the 150- to 180-degree region in all five cases (Table 2). No correlation was found between anatomic measurements and force metrics or between anatomic measurements and traumatism (Table 3) (NS, Mann–Whitney *U*-test).

3.1 Atraumatic insertions

The overall insertion force profile was similar for all temporal bones; the frictional forces remained low for the first half of the insertion and then rose continuously reaching a peak force at the end of the insertion (59.4 ± 19.9 mN). In the region at risk for translocation (150 degrees), all apart from one atraumatic insertion had lower frictional forces than the traumatic insertions (Fig. 4). **An incomplete insertion occurred (specimen 4G, one electrode out), but no obvious intracochlear obstacle was found at histological exam.**

3.2 Traumatic insertions

Analysis of the frictional force profiles in the traumatic insertions showed an irregular profile in four insertions and the presence of a peak (peak force: 29.56 ± 18.2 mN) around 15 seconds after the beginning of insertion corresponding approximately to the moment when the tip of the array impacted with the lateral wall of the cochlea in the 150- to 180-degree region; another insertion presented an early rise of force (see Fig. 3). The last traumatic insertion had a smooth and regular force profile.

The insertion force profile in the region 90–240 degrees for all of the cochleae is reported in Fig. 4. As clearly seen from the force curves, the insertion force increased significantly as a function of depth of insertion both in traumatic and atraumatic insertions ($r = 0.57$, $p < 0.001$). Nevertheless, the two groups had significantly different force values at different depths of insertion ($p < 0.001$, two-way ANOVA), and the slopes of the regression lines for the atraumatic ($y = 1.34x + 0.7$) and traumatic ($y = 3.37x + 0.84$) insertions were significantly different ($p < 0.001$, ANCOVA) (Fig. 4).

Three insertions had a maximum peak force above 0.1 N and this was always associated with scalar translocation, nevertheless, no difference in force was found between different grades of trauma (i.e. grade 4 vs grade 3). No other correlation was found between other force metrics and inner ear traumatism.

An incomplete insertion occurred in one cochlea (specimen 6D). In this specimen, a trauma occurred at 180-degrees, four electrodes were translocated to the scala vestibuli and two electrodes were outside the cochlea.

4. Discussion

The preservation of inner ear structures and consequently, the preservation of residual hearing during cochlear implantation depend mainly on the surgical technique used and on the characteristics of the electrode array. Post-insertional intracochlear fibrosis may be reduced by limiting insertion traumatism and increasing the biocompatibility of the electrodes. A correlation

between word recognition score and intracochlear new bone and fibrous tissue formation after cochlear implantation has recently been demonstrated (Kamakura and Nadol, 2016).

In the present temporal bone study, a long (28 mm) lateral wall array was used and a relationship has been found between the insertion force profile and preservation of inner ear structure. To the best of our knowledge, this represents the first report showing a direct correlation between the insertion forces and intracochlear traumatism. Nevertheless, our cadaveric model has some limitations and the intracochlear electrode array insertions cannot be strictly compared to in vivo studies. In this experimental set-up, the temporal bones were frozen and unfrozen multiple times for specimen preparation, imaging and array insertion. This probably interfered with the stiffness and resistance of the inner ear structures (spiral ligament, basilar membrane, spiral osseous lamina). All of the insertions were made via an extended round window (ERW) approach to standardize the insertion **and reduce the anatomical variation of the hook region of the cochlea that is reported to be wide (Atturo et al., 2014). Moreover, the choice of this approach was made in order to limit the artifact of measurement of the force determined by the friction between the electrode array and the anterior rim of the round window and with the crista fenestra**. Wanna et al. (2015) reported that ERW insertion and cochleostomy were more traumatic and prone to scalar translocation than pure round window insertion. **Different electrode designs or different entry points into the cochlea have a different trajectory and different impact on the modiolar or lateral wall region (Zhou et al. 2015).** The choice of entry point in the cochlea should be made on the basis of the anatomical variation of the cochlea (Atturo et al., 2014) and the electrode array should be chosen as a consequence; in any case, round window insertion should be avoided in the case of perimodiolar array use (Jeyakumar et al., 2014). Although electrode insertion trauma is influenced by array design, the occurrence of severe trauma **using straight electrodes** is mainly reported in the region of 180-degrees. This is caused in part by the decrease in diameter of the scala vestibule at this point (Biedron et al., 2010) and by the fact that lateral wall electrodes directly impact on that region in the case of ERW or cochleostomy insertion **(Zhou et al. 2015)**.

Several studies have been published describing cochlear implant insertion related trauma. The earliest study by Kennedy (1987), which evaluated a straight electrode array inserted through an ERW approach, reported that insertion beyond the point of first resistance resulted in damage to the spiral ligament, the basilar membrane, and osseous spiral lamina at the junction between the first and second half of the first turn. Welling et al. (1993) reported the results of a temporal bone study on the insertional trauma of different electrode arrays available at that time finding damage to the lateral wall structures of the cochlea in all three of the arrays tested, but no traumatism to the modiolar region**. Indeed**, **a post-mortem histologic study in an implanted patient showed that**

postoperative bone formation was located in the ascending limb of the basal turn (Nadol et al. 2001), corresponding to the location of the trauma found in the present study. More recently, Adunka and Kiefer (2006) evaluated the basal trauma in temporal bone insertions of Med El arrays of different length. Using a round window approach, rupture of the spiral osseus lamina was reported in 2/8 specimens, whereas a deeper insertion (24-30 mm with a Flex soft electrode) was reported to be more traumatic. Other groups reported their experience with a different straight array, the Cochlear SRA (currently the Cochlear CI422 array). This electrode was atraumatic in shallow insertions (i.e. up to 20 mm) but more traumatic in deeper insertions (Skarzynski et al., 2012; Mukherjee et al., 2012). All these studies reported a subjective force measurement and suggested stopping the insertion at the point of first resistance in procedures aiming for hearing preservation.

The resistance of the inner ear structures has been studied previously in fresh cadaveric temporal bones. Ishii et al. (1995) isolated the basilar membrane and measured the rupture force as between 29 and 39 mN, whereas for only the membrane of Reissner, the authors measured a force of 4.2 mN. Schuster et al. (2015) reported that the mean value of the force necessary to rupture the entire system including the basilar membrane, Reissner's membrane and lamina spiralis ossea was 88 mN, and values ranged from 42 to 122 mN. In these studies, the forces applied were perpendicular to the basilar membrane; this situation was not comparable with the force applied during electrode array insertion as the vector of the force may differ (Roland, 2005). A measure of the forces during CI insertion have been made by Rohani et al. (2014) who studied the insertion profile of three different electrodes in six fresh temporal bones. In that study, the array was inserted through a tunnel drilled in the mastoid with a preimplantation planned linear trajectory without performing a mastoidectomy, and incomplete insertions of Med El Standard arrays were obtained.

A previous study in our lab (Nguyen et al., 2012) reported a correlation between different curved array profiles and quality of insertion. That study identified a peak force of 0.5 N with a slope increase after 10 mm in an incomplete insertion, and a peak force of 0.3 N and a rise in slope after only 7 mm in one insertion having a folding tip; in that study, histologic analysis of inner ear traumatism was not performed, and the correlation between forces and traumatism was not analyzed. Several studies have reported the average force during cochlear implantation (Schurzig et al., 2010; Kontorinis et al., 2011 a; Rohani et al., 2014). This metric depends on the duration of insertion and was extremely low in protracted insertions with several stops and starts and long pauses even if a high peak force occurred during the insertion. We believe the most reasonable value to be considered should be the peak force. Indeed, in the present study, the only metric of insertion that correlated with insertion trauma was peak force. In 11 out of 12 insertions, the maximal peak force occurred at the end of the insertion and represented the frictional force of the entire array with

the lateral cochlear wall and inner ear structures. The force value in the region of first contact of the tip of the array with the cochlear structures should represent the value to monitor during electrode insertion so as to be able to detect and avoid complications. In the case of elevation of the force over a defined threshold in the first contact region, the insertion technique should be modified. A small rotation of the electrode or a backward and forward movement while monitoring the forces could be the correct procedure to use to avoid structure trauma. Indeed, steerable (Zhang et al., 2010) or curvature controlled (Wu et al., 2005) electrode arrays have been proposed to reduce the frictional forces. **The use of vibration has been studied in mechanics in order to reduce the frictional forces between two surfaces (Tsai et al 2006) but, to our knowledge, this has not yet been applied in cochlear implant surgery. Other factors have been studied by several authors to reduce trauma during cochlear implantation. The use of a lubricant such as hyaluronic acid or glycerin has been demonstrated to reduce the frictional forces during cochlear implant insertion (Zhang et al. 2009, Kontorinis et al. 2011b, Miroir et al 2011). A low speed of insertion would positively influence residual hearing preservation (Kontorinis et al. 2011a, Rajan et al 2013).**

Considering different array designs, the advance off stylet technique for a perimodiolar precurved electrode has been demonstrated to be associated with lower average and maximum insertion forces, compared to traditional insertion of the same array (Schurzig et al. 2010).

In our results, the frictional forces for traumatic and atraumatic insertion were already different at 90-degrees insertion depth, before translocation and contact of the tip of the array with the cochlear lateral wall in the region at risk for traumatism. One might suppose that other factors may influence the scalar translocation. The axis of insertion of the array, which should be tangential to the basal turn of the cochlea (Briggs et al., 2011), was not controlled in our study and was determined by the position of the facial nerve in the posterior tympanotomy, indeed, in most cases, the ideal insertion vector coaxial to the centerline of the scala tympani is interrupted by the facial nerve (Meshik et al., 2010). A preoperatively planned axis of insertion guided by a surgical navigation system could possibly improve inner ear structure preservation by aligning the electrodes array with the most appropriate insertion axis (Torres et al., 2016 a, b).

The translocation rate found in this study was unexpectedly high but similar to other frozen temporal bone studies. Martins et al. (2015) found a higher rate of traumatism (36%) in the region 180-270 degrees than in other cochlear segments. This may be related to the quality of inner ear structures possibly modified by the freeze-thaw cycle. These findings cannot be directly compared with cochlear implant reports on patients implanted with the same electrode array. Indeed, the radiological translocation rate in patients was reported to be significantly lower than our findings in temporal bone (Boyer et al. 2015, Nordfalk et al, 2016). Nevertheless, we believe that the

present temporal bone model allowed the identification of the area at risk for trauma and translocation, and quantified the forces responsible for a trauma.

4.1 Conclusion

In this study, the **insertion forces of a long straight electrode array inserted via an extended round window approach** were correlated with inner ear structure damage **in the temporal bone model**. Moreover, the region at 150- to 180-degrees represented the region at risk for scalar translocation and a high peak force in this area corresponded to basilar membrane lesion or translocation. Two different sets of values were obtained for traumatic and atraumatic insertions; these values, if confirmed by further studies **in patients**, could be useful for the future development of a force feedback CI insertion tool to reduce the risk of insertion-related damage and to provide the best chance for optimal hearing rehabilitation in cochlear implanted patients.

REFERENCES

1. Adunka, O., Kiefer, J., 2006. Impact of electrode insertion depth on intracochlear trauma. Otolaryngology and Head and Neck Surgery 135(3), 374-382.
2. Aschendorff, A., Kromeier, J., Klenzner, T., Laszig, R., 2007. Quality control after insertion of the nucleus contour and contour advance electrode in adults. Ear and Hearing 28(2 Suppl), 75S-79S.
3. Atturo, F., Barbara, M., Rask-Andersen, H., 2014. On the anatomy of the 'hook' region of the human cochlea and how it relates to cochlear implantation. Audiology & Neuro-otology 19, 378-385.
4. Biedron, S., Prescher, A., Ilgner, J., Westhofen, M., 2010. The internal dimensions of the cochlear scalae with special reference to cochlear electrode insertion trauma. Otology & Neurotology 31, 731-737.
5. Boyer, E., Karkas, A., Attye, A., Lefournier, V., Escude, B., Schmerber, S., 2015. Scalar localization by cone-beam computed tomography of cochlear implant carriers: a comparative study between straight and periomodiolar precurved electrode arrays. Otology & Neurotology 36, 422-429.
6. Briggs, R.J., Tykocinski, M., Xu, J., Risi, F., Svehla, M., Cowan, R., Stover, T., Erfurt, P., Lenarz, T., 2006. Comparison of round window and cochleostomy approaches with a prototype hearing preservation electrode. Audiology & Neuro-otology 11 Suppl 1, 42-48.
7. Briggs, R.J., Tykocinski, M., Lazsig, R., Aschendorff, A., Lenarz, T., Stöver, T., Fraysse, B., Marx, M., Roland, J.T. Jr, Roland, P.S., Wright, C.G., Gantz, B.J., Patrick, J.F., Risi, F., 2011. Development and evaluation of the modiolar research array--multi-centre collaborative study in human temporal bones. Cochlear Implants International 12, 129-139.
8. Carlson, M.L., Driscoll, C.L., Gifford, R.H., Service, G.J., Tombers, N.M., Hughes-Borst, B.J., Neff, B.A., Beatty, C.W., 2011. Implications of minimizing trauma during conventional cochlear implantation. Otology & Neurotology 32, 962-968.
9. Doshi, J., Johnson, P., Mawman, D., Green, K., Bruce, I.A., Freeman, S., Lloyd, S.K., 2015. Straight versus modiolar hugging electrodes: does one perform better than the other? Otology & Neurotology 36, 223-227.
10. De Seta, D., Nguyen, Y., Bonnard, D., Ferrary, E., Godey, B., Bakhos, D., Mondain, M., Deguine, O., Sterkers, O., Bernardeschi, D., Mosnier, I., 2016. The role of electrode placement

in bilateral simultaneously cochlear-implanted adult patients. Otolaryngology and Head and Neck Surgery 155, 485-493.

11. Escudé, B., James, C., Deguine, O., Cochard, N., Eter, E., Fraysse, B., 2006. The size of the cochlea and predictions of insertion depth angles for cochlear implant electrodes. Audiology & Neuro-otology 11 Suppl 1, 27-33.
12. Eshraghi, A.A., Lang, D.M., Roell, J., Van De Water, T.R., Garnham, C., Rodrigues, H., Guardiola, M., Gupta, C., Mittal, J., 2015. Mechanisms of programmed cell death signaling in hair cells and support cells post-electrode insertion trauma. Acta Oto-laryngologica 135, 328-334.
13. Holden, L.K., Finley, C.C., Firszt, J.B., Holden, T.A., Brenner, C., Potts, L.G., Gotter, B.D., Vanderhoof, S.S., Mispagel, K., Heydebrand, G., Skinner, M.W., 2013. Factors affecting open-set word recognition in adults with cochlear implants. Ear and Hearing 34, 342-360.
14. Hunter, J.B., Gifford, R.H., Wanna, G.B., Labadie, R.F., Bennett, M.L., Haynes, D.S., Rivas, A., 2016. Hearing preservation outcomes with a mid-scala electrode in cochlear implantation. Otology & Neurotology 37, 235-240.
15. Ishii, T., Takayama, M., Takahashi, Y., 1995. Mechanical properties of human round window, basilar and Reissner's membranes. Acta Oto-laryngologica 519, 78-82.
16. Jeyakumar, A., Peña, S.F., Brickman, T.M., 2014. Round window insertion of precurved electrodes is traumatic. Otology & Neurotology 35, 52-57.
17. Kamakura, T., Nadol, J.B. Jr, 2016. Correlation between word recognition score and intracochlear new bone and fibrous tissue after cochlear implantation in the human. Hearing Research Jun 29. pii: S0378-5955(16)30135-6. doi: 10.1016/j.heares.2016.06.015.
18. Kennedy, D.W., 1987. Multichannel intracochlear electrodes: mechanism of insertion trauma. Laryngoscope 97, 42-49.
19. Kontorinis, G., Lenarz, T., Stöver, T., Paasche, G., 2011a. Impact of the insertion speed of cochlear implant electrodes on the insertion forces. Otology & Neurotology 32, 565-570.
20. Kontorinis, G., Paasche, G., Lenarz, T., Stöver, T., 2011b. The effect of different lubricants on cochlear implant electrode insertion forces. Otology & Neurotology 32, 1050-1056.
21. Lehnhardt, E., 1993. Intracochlear placement of cochlear implant electrodes in soft surgery technique. Deutsche Gesellschaft der Hals- Nasen- und Ohrenärzte; Zeitschaft für Nasen- und Ohrenheilkunde 41, 356-359.
22. Lenarz, T., Stover, T., Buechner, A., Paasche, G., Briggs, R., Risi, F., Pesch, J., Battmer, R.D., 2006. Temporal bone results and hearing preservation with a new straight electrode. Audiology & Neuro-otology 11 Suppl 1, 34-41.

23. Majdani, O., Schurzig, D., Hussong, A., Rau, T., Wittkopf, J., Lenarz, T., Labadie, R.F., 2010. Force measurement of insertion of cochlear implant electrode arrays in vitro: comparison of surgeon to automated insertion tool. Acta Oto-laryngologica 130, 31-36.
24. Martinez-Monedero, R., Niparko, J.K., Aygun, N., 2011. Cochlear coiling pattern and orientation differences in cochlear implant candidates. Otology & Neurotology 32, 1086-1093.
25. Martins Gde, S., Brito Neto, R.V., Tsuji, R.K., Gebrim, E.M., Bento, R.F., 2015. Evaluation of intracochlear trauma caused by insertion of cochlear implant electrode arrays through different quadrants of the round window. BioMed Research International 2015, 236364.
26. Meshik, X., Holden, T.A., Chole, R.A., Hullar, T.E., 2010. Optimal cochlear implant insertion vectors. Otology & Neurotology 31, 58-63.
27. Miroir, M., Nguyen, Y., Kazmitcheff, G., Ferrary, E., Sterkers, O., Grayeli, A.B., 2012. Friction force measurement during cochlear implant insertion: application to a force-controlled insertion tool design. Otology & Neurotology 33, 1092-1100.
28. Mukherjee, P., Uzun-Coruhlu, H., Wong, C.C., Curthoys, I.S., Jones, A.S., Gibson, W.P., 2012. Assessment of intracochlear trauma caused by the insertion of a new straight research array. Cochlear Implants International 13, 156-162.
29. Nordfalk, K.F., Rasmussen, K., Hopp, E., Bunne, M., Silvola, J.T., Jablonski, G.E., 2016. Insertion depth in cochlear implantation and outcome in residual hearing and vestibular function. Ear and Hearing 37, 129-137.
30. Nguyen, Y., Miroir, M., Kazmitcheff, G., Sutter, J., Bensidhoum, M., Ferrary, E., Sterkers, O., Bozorg Grayeli, A., 2012. Cochlear implant insertion forces in microdissected human cochlea to evaluate a prototype array. Audiology & Neuro-otology 17, 290-298.
31. Nguyen, Y., Mosnier, I., Borel, S., Ambert-Dahan, E., Bouccara, D., Bozorg-Grayeli, A., Ferrary, E., Sterkers, O., 2013. Evolution of electrode array diameter for hearing preservation in cochlear implantation. Acta Oto-laryngologica 133, 116-122.
32. Nguyen, Y., Kazmitcheff, G., De Seta, D., Miroir, M., Ferrary, E., Sterkers, O., 2014. Definition of metrics to evaluate cochlear array insertion forces performed with forceps, insertion tool, or motorized tool in temporal bone specimens. BioMed Research International 2014, 532-570.
33. Nguyen, Y., Bernardeschi, D., Kazmitcheff, G., Miroir, M., Vauchel, T., Ferrary, E., Sterkers, O., 2015. Effect of embedded dexamethasone in cochlear implant array on insertion forces in an artificial model of scala tympani. Otology & Neurotology 36, 354-358.

34. Rajan, G.P., Kontorinis, G., Kuthubutheen, J., 2013. The effects of insertion speed on inner ear function during cochlear implantation: a comparison study. Audiology & Neuro-otology 18, 17-22.
35. Rohani, P., Pile, J., Kahrs, L.A., Balachandran, R., Blachon, G.S., Simaan, N., Labadie, R.F., 2014. Forces and trauma associated with minimally invasive image-guided cochlear implantation. Otolaryngology and Head and Neck Surgery 150, 638-645.
36. Roland, J.T. Jr., 2005. A model for cochlear implant electrode insertion and force evaluation: results with a new electrode design and insertion technique. Laryngoscope 115, 1325-1339.
37. Schurzig, D., Webster, R.J. 3rd, Dietrich, M.S., Labadie, R.F., 2010. Force of cochlear implant electrode insertion performed by a robotic insertion tool: comparison of traditional versus Advance Of-Stylet techniques. Otology & Neurotology 31:1207-10.
38. Schuster, D., Kratchman, L.B., Labadie, R.F., 2015. Characterization of intracochlear rupture forces in fresh human cadaveric cochleae. Otology & Neurotology 36, 657-661.
39. Skarzynski, H., Lorens, A., Matusiak, M., Porowski, M., Skarzynski, P.H., James, C.J., 2012. Partial deafness treatment with the nucleus straight research array cochlear implant. Audiology & Neuro-otology 17, 82-91.
40. Skinner, M.W., Holden, T.A., Whiting, B.R., Voie, A.H., Brunsden, B., Neely, J.G., Saxon, E.A., Hullar, T.E., Finley, C.C., 2007. In vivo estimates of the position of advanced bionics electrode arrays in the human cochlea. The Annals of Otology, Rhinology & Laryngology. Supplement 197, 2-24.
41. Torres, R., Kazmitcheff, G., Bernardeschi, D., De Seta, D., Bensimon, J.L., Ferrary, E., Sterkers, O., Nguyen, Y., 2016a. Variability of the mental representation of the cochlear anatomy during cochlear implantation. European Archives of Otorhinolaryngology 273, 2009-2018.
42. Torres, R., Kazmitcheff, G., De Seta, D., Ferrary, E., Sterkers, O., Nguyen, Y., 2016b. Improvement of the insertion axis for cochlear implantation with a robot-based system. European Archives Otorhinolaryngology Oct 4. PMID: 27704279.
43. Tsai, C., Tseng, C., 2006. The effect of friction reduction in the presence of in-plane vibrations. Archive of Applied Mechanics 75, 164-176.
44. Wanna, G.B., Noble, J.H., McRackan, T.R., Dawant, B.M., Dietrich, M.S., Watkins, L.D., Rivas, A., Schuman, T.A., Labadie, R.F., 2011. Assessment of electrode placement and audiological outcomes in bilateral cochlear implantation. Otology & Neurotology 32, 428-432.
45. Wanna, G.B., Noble, J.H., Gifford, R.H., Dietrich, M.S., Sweeney, A.D., Zhang, D., Dawant, B.M., Rivas, A., Labadie, R.F., 2015. Impact of intrascalar electrode location, electrode type, and angular insertion depth on residual hearing in cochlear implant patients: preliminary results. Otology & Neurotology 36, 1343-1348.

46. Welling, D.B., Hinojosa, R., Gantz, B.J., Lee, J.T., 1993. Insertional trauma of multichannel cochlear implants. Laryngoscope 103, 995-1001.
47. Wu, J., Yan, L., Xu, H., Tang, W.C., Zeng, F.G., 2005. A curvature-controlled 3D micro-electrode array for cochlear implants. Proceedings of 13th International Conference Solid-State Sensors, Actuators and Microsystems, Seoul, Korea, 1636–1639.
48. Xu, J., Xu, S.A., Cohen, L.T., Clark, G.M., 2000. Cochlear view: postoperative radiography for cochlear implantation. The American Journal of Otology 21, 49-56.
49. Zhang, J., Bhattacharyya, S., Simaan, N., 2009. Model and parameter identification of friction during robotic insertion of cochlear-implant electrode arrays. 2009 IEEE International Conference on Robotics and Automation, Kobe, Japan, pp. 3859‑3864.
50. Zhang, J., Wei, W., Ding, J., Roland, J.T. Jr, Manolidis, S., Simaan, N., 2010. Inroads toward robot-assisted cochlear implant surgery using steerable electrode arrays. Otology & Neurotology 31, 1199-1206.
51. Zhou, L., Friedmann, D.R., Treaba, C., Peng, R., Roland, J.T. Jr, 2015. Does cochleostomy location influence electrode trajectory and intracochlear trauma? Laryngoscope 125, 966-971.

TABLE I. PRE- AND POST-INSERTION MEASUREMENTS

Anatomical parameters	
Distance A (mm)	9.0±0.42
Cochlear height (mm)	3.2±0.30
Angle between 1st and 2nd turn (degrees)	14.8±1.36
Insertion force parameters	
Maximum peak force (mN)	71.3±30.3
Force momentum (N·s)	418.55±95
Jerk (N·s^{-1})	200.02±48
Sudden rise (No)	50.3±30

TABLE II. TRAUMATIC INSERTIONS: HISTOLOGY

Specimen #	Scalar translocation (degrees)	Translocated electrodes (n)	Cochlear trauma scale Location (degrees)	
			(0-180)	(181-360)
R1G	150	5	4	3
R3G	-	-	2	2
R4D	150	5	3	3
R5D	190	2	2	3
R6D	180	4	3	3
R6G	160	5	4	4

TABLE III. ANATOMICAL MEASUREMENTS IN TRAUMATIC AND ATRAUMATIC INSERTIONS

	Distance A (mm)	Height (mm)	Angle 1st-2nd turn (degrees)	Vertical diameter 180° (mm)	Horizontal diameter 180° (mm)	Vertical diameter 360° (mm)	Horizontal diameter 360° (mm)
Traumatic insertions (n=6; mean ± SD)	9.1±0.52	3.2±0.36	14.7±1.17	1.5±0.16	1.7±0.16	1.5±0.10	1.5±0.15
Atraumatic insertions (n=6; Mean ± SD)	9.1±0.33	3.3±0.22	14.9±1.64	1.7±0.15	1.7±0.14	1.6±0.10	1.6±0.08

Figures legend

Figure 1. Pre-insertion cone beam CT measurements. A. The major cochlear diameter was measured in the cochlear view. The superior semicircular canal (SSC) plane was used as the reference plane. B. The cochlear height was measured in the plane perpendicular to the SSC passing through the modiolus in the cochlear view. C. The cochlear lumen diameters were measured in the mid-modiolar plane at 180- and 360-degrees. D. The angle between the 1^{st} and 2^{nd} turn was measured in the plane parallel to the SSC.

Figure 2. Measurement insertion bench. The insertion tool was fixed to a steady flexible arm, avoiding any contact with the cochlea. The insertion speed was $0.8\ mm{\cdot}s^{-1}$. The insertion forces were measured with a 6-axis force sensor (small panel) and subsequently analyzed.

Figure 3. The upper three panels show a scanning electron microscope image, light microscope image and insertion force profile of an atraumatic insertion. Below this, the other panels show three different traumatic insertions. The fracture of the osseus spiral lamina (OSL) at 160 degreesis visible both in the SEM and the light microscope image (thick arrows). A peak force (thin arrows) is visible 15 seconds after the beginning of the insertion, corresponding to traumatism at 160 degrees. An early scalar translocation corresponding to an early rise of force occurred in the first part of the insertion. BM, basilar membrane, OSL, osseous spiral lamina.

Figure 4. Frictional force profile of traumatic (in red) and atraumatic (in green) insertions in the critical region for translocation (90-240°). All of the traumatism occurred between 150° and 180°. The dashed lines represent the linear regression lines for traumatic ($y=3.37x+0.84$) and atraumatic ($y=1.34x+0.69$) insertion.

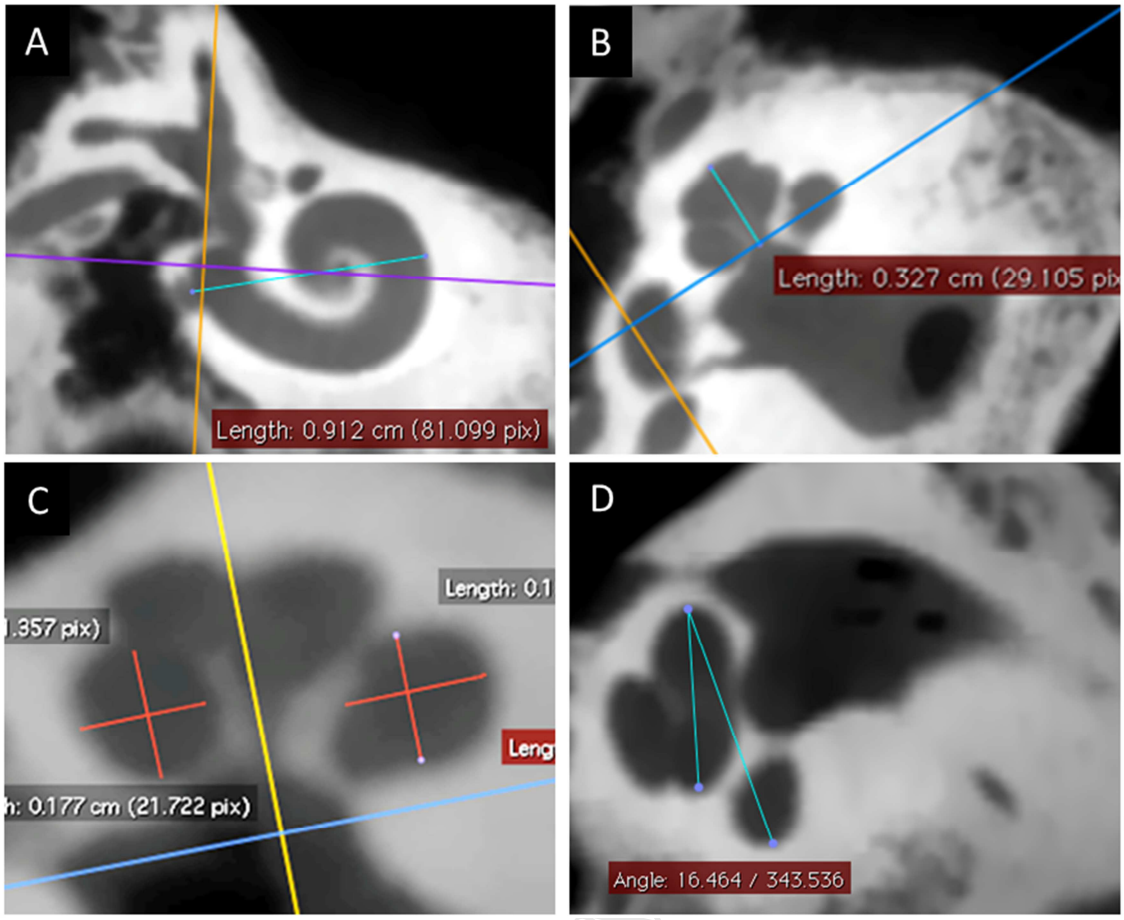

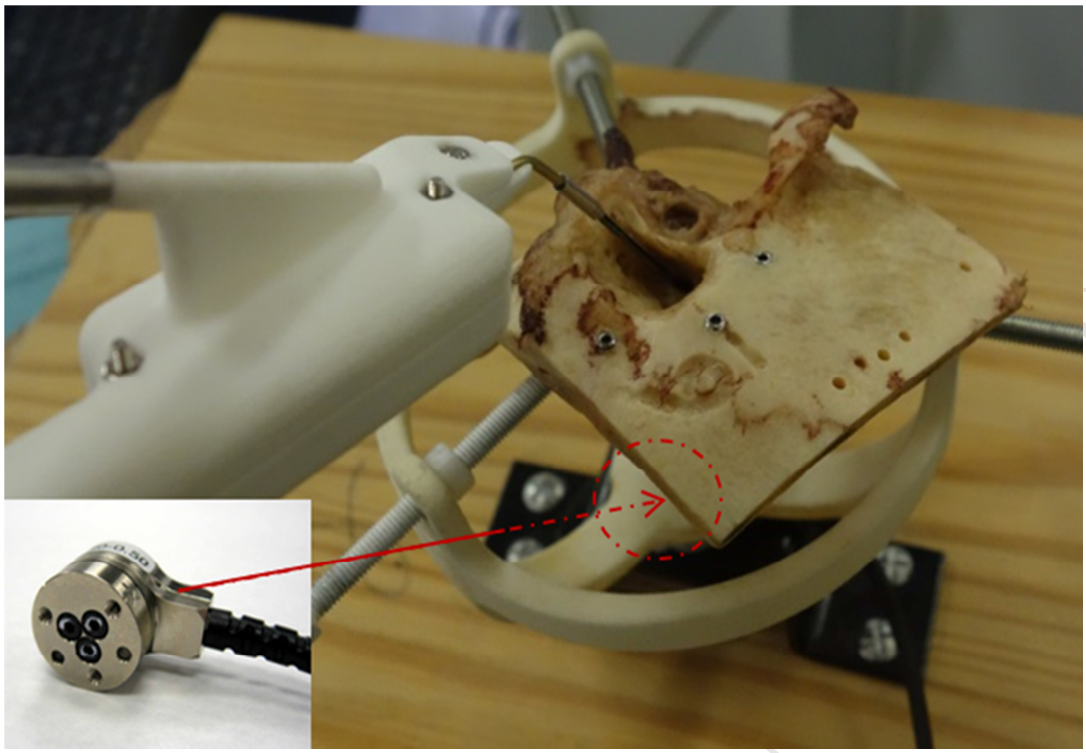

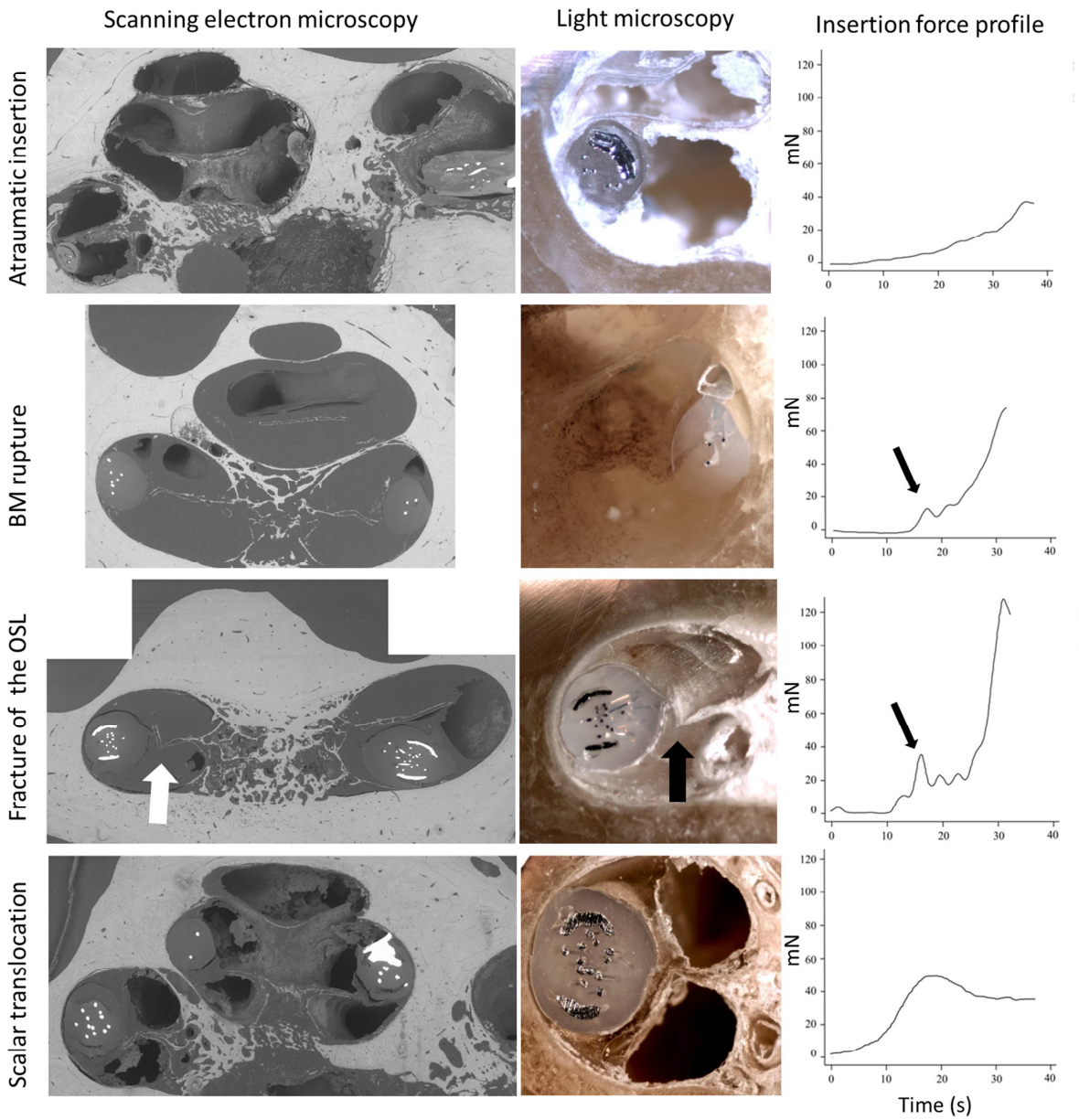
Scanning electron microscopy
Light microscopy
Insertion force profile
Atraumatic insertion
BM rupture
Fracture of the OSL
Scalar translocation
mN
Time (s)

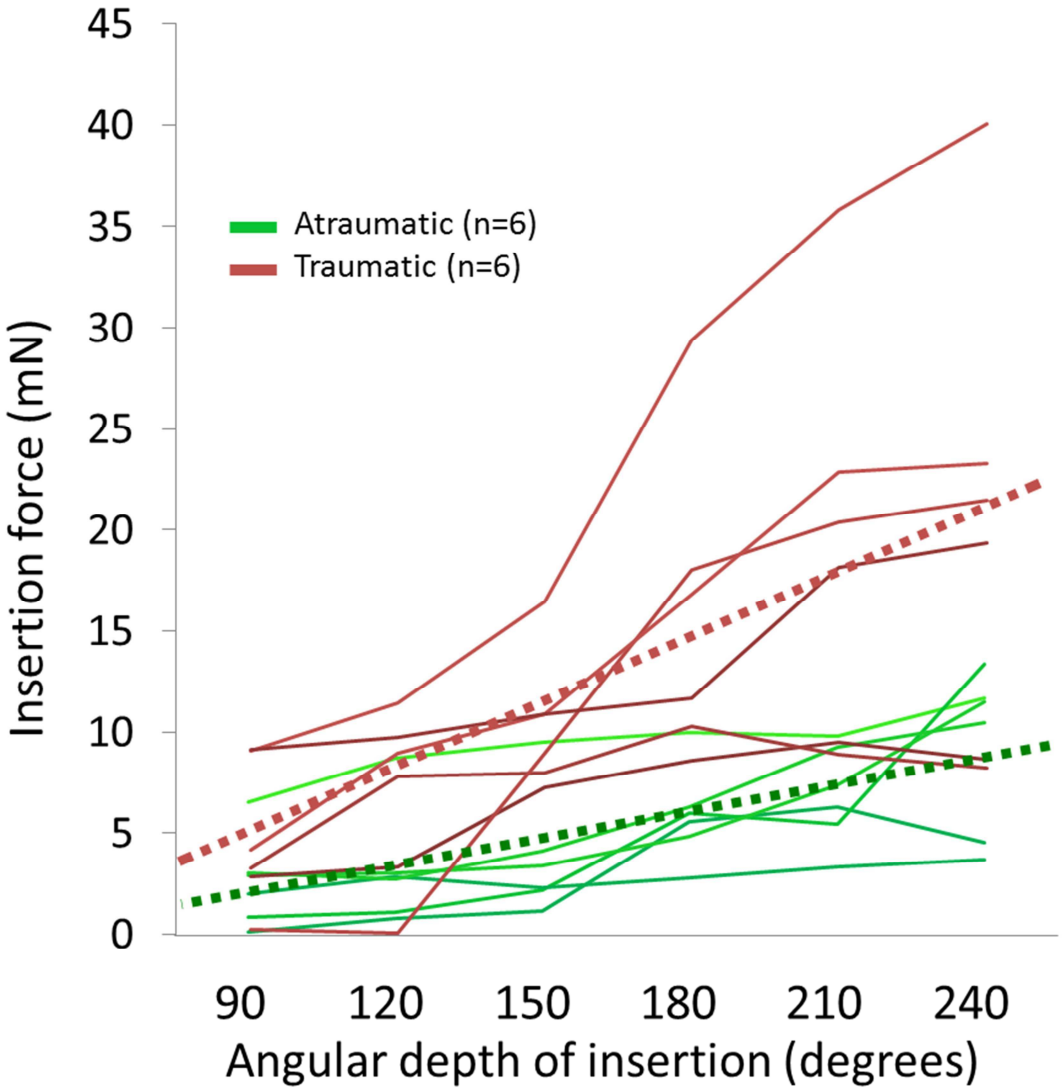
45
40
35
30
25
20
15
10
5
0
Insertion force (mN)
Atraumatic (n=6)
Traumatic (n=6)
90
120
150
180
210
240
Angular depth of insertion (degrees)

- Twelve human cadaveric temporal bones were cochlear implanted at constant speed of insertion
- Insertion forces during cochlear implantation were correlated with inner ear structure traumatism
- Two different functions were identified for traumatic and atraumatic insertions
- The control of the insertion force could reduce the risk of insertion-related damage